Int. J. Heat Mass Transfer. Vol. 16, pp. 359–369. Pergamon Press 1973. Printed in Great Britain

EFFECTS OF UPSTREAM AND DOWNSTREAM BOUNDARY CONDITIONS ON HEAT (MASS) TRANSFER WITH AXIAL DIFFUSION

YEHUDA TAITEL

School of Engineering, Tel Aviv University, Ramat-Aviv, Israel

and

M. BENTWICH and ABRAHAM TAMIR

Faculty of Engineering Sciences, University of the Negev, Beer-Sheva, Israel

(*Received* 15 *February* 1972 *and in revised form* 31 *May* 1972)

Abstract—The authors investigate systematically the role of upstream and downstream boundary conditions on the heat (or mass) transfer when axial diffusion is effective. As examples, three similar cases of plug flow in channels flows are studied. In all cases there is a central heating section and the fluid flows from there into an insulated semi-infinite conduit. The situations prevailing upstream of this section vary.

As expected it is found that these situations have a substantial influence when the Péclét number is low, and the heating section is short.

The analysis is carried out assuming a uniform profile. It is, nevertheless, less than straightforward because in all three cases the boundary conditions are mixed. Solutions are obtained in the form of Fourier Integrals the inversion of which is carried out numerically.

NOMENCLATURE

a, a constant, used for lower limit of integration;
A, a function, equation (11);
b, dimensionless length of the heating section, $Bp/2L$;
B, axial length of the heating section, also a function, equation (11′);
C_p, heat capacity at constant pressure;
c, a constant, used for upper limit of integration;
f, transformed dimensionless flux at $y = p/2$;
h, heat transfer coefficient;
H, matrix or vector, equations (A.4), (A.6) and (A.7);
i, index of the finite difference subdivisions, also the symbol for imaginary numbers;
j, index of the finite difference subdivisions;
k, thermal conductivity;
K, kernel;
L, half width of the channel;
Nu, Nusselt number, hL/k;
p, Péclét number, $\rho UC_pL/k$;
q, heat flux;
Q, rate of heat transferred;
r, the variable $|x - \xi|$ or $|x + \xi|$, equations (A.5) and (A.7);
S, area;
T, local temperature;
u, dimensionless dependent variable, $\phi \exp(-x)$;
U, velocity;
x, dimensionless coordinate, $Xp/2L$;
X, axis along stream lines (Fig. 1);
y, dimensionless coordinate, $Yp/2L$;
Y, axis perpendicular to streamlines (Fig. 1);
β_n, $\sqrt{(1 + 4n^2\pi^2/p^2)}$;
η, variable of integration;
λ, variable of integration;

ξ, variable of integration;
ρ, density;
ϕ, dimensionless temperature.

Subscripts and superscripts
m, running index;
n, running index;
w, at the heating walls;
0, inlet conditions;
-, average.

INTRODUCTION

MOST of the available analytic studies of conductive–convective heat (or mass) transfer patterns are restricted to high Péclét numbers. These analyses are based on the assumption that the term which represents axial conduction in the diffusion equation, $\partial^2 T/\partial X^2$, is negligible. Here, $T(X,Y)$ is the temperature distribution, (X, Y) are Cartesian co-ordinates and the flow is X directed. However if the Péclét number is low that term cannot be omitted. Its inclusion requires careful consideration of both the upstream and downstream boundary conditions. It seems that the effects of these has been somewhat overlooked. The role of these conditions when axial diffusion is effective is investigated in this work by considering and then comparing various heat and mass concentration distributions in a channel plug flow.

The physical models considered are outlined in Fig. 1. These consist of an infinite or semi-infinite channels with their central section exposed to a heating surface. On the latter either the temperature, T_w, or else the heat flux, q_w, is prescribed. Both T_w, and q_w, are assumed to be uniform. From the heated section the fluid flows into an insulated semi-infinite conduit. The situations prevailing upstream of the heating section vary from case to case. In model (i) the fluid enters the heated section through a semi-infinite insulated duct. The temperature at $X = -\infty$ is T_0. This model is the appropriate representation for exchangers in which the fluid is guided into and out of the exchange-section through long insulated conduits. Model (ii)

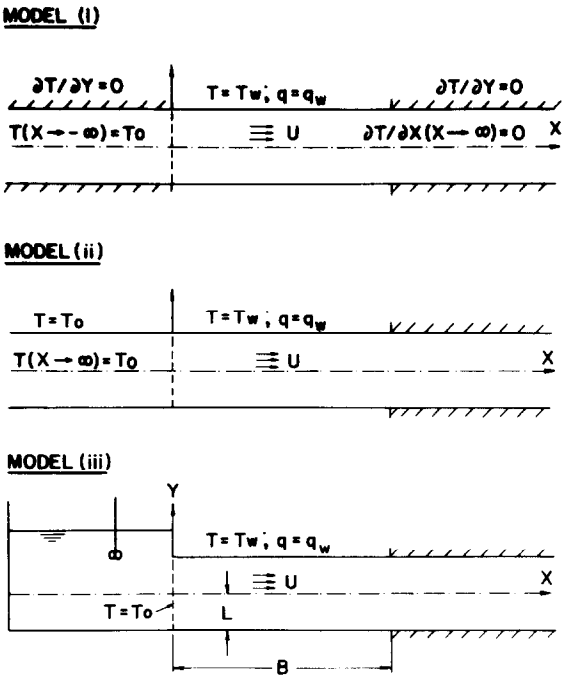

FIG. 1. Physical model and boundary conditions of the three representative models.

represents exchangers in which the fluid undergoes preheating before entering the main part of the exchanger. Thus in model (ii) the entire surface of the duct upstream of the heating section is kept at a constant temperature T_0. In model (iii) the incoming fluid enters the heated section straight from a well mixed container in which the prevailing temperature is T_0.

Note that although these three models represent a good number of physically realizable situations, when axial diffusion is ignored the differences between the situations prevailing upstream have no impact on the transfer patterns. Indeed if the term $\partial^2 T/\partial X^2$ of the diffusion equation is omitted then the upstream boundary conditions at the entrance to the heating section reads $T = T_0$ at $X = 0$ in all three cases. The results obtained here show that the transfer patterns vary from model to model.

Discussions of the effects of axial diffusion in a channel or pipe flow have appeared in the

literature. Cases in which the upstream condition is that of model (iii) were treated by Rotem [1], Singh [2], Boyadzhiev [3], Hsu [4] and Schneider [5]. Situations in which there is upstream heating or insulated incoming conduits as in models (ii) and (i), respectively, are discussed by Schneider [5], Hsu [6,7] and Jones [8]. Note that in the works cited the heating section is infinitely long. Therefore, unlike these, the proposed analysis reveals the combined influence of the upstream and downstream condition. Although the authors restrict themselves to the simple geometry of two dimensional channel with uniform velocity profile (plug flow), the problems under discussion is still mathematically difficult because the imposed boundary conditions are mixed. However it is expected that the relative effect of the different boundary conditions will be similar also for pipe flow and other ducts with non uniform profiles.

FORMULATION

In all three cases the energy equation reads

$$\rho C_p U \frac{\partial T}{\partial X} = k\left(\frac{\partial^2 T}{\partial X^2} + \frac{\partial^2 T}{\partial Y^2}\right) \qquad (1)$$

where (X, Y) are Cartesian co-ordinates, U is the velocity of the stream, k is the conductivity of the liquid, and C_p is its heat capacity. When use is made of the following transformations

$$(x,y) \equiv (X,Y)p/2L \qquad u \equiv \exp(-x)\phi$$

$\phi \equiv (T - T_0)/(T_w - T_0)$ if the temperature is prescribed

$\phi \equiv k(T - T_0)p/2q_wL$ if the flux is prescribed

equation (1) reduces to the following so called Helmholtz equation

$$\left(\frac{\partial^2}{\partial x^2} + \frac{\partial^2}{\partial y^2}\right)u = u. \qquad (2)$$

Here L is half the width of the channel and p is the Péclét number which is defined thus:

$$p \equiv \rho U C_p L/k.$$

When the temperature rather than the flux is prescribed along the heating section, the following boundary conditions hold for all three models,

$$\partial u/\partial y = 0 \qquad y = 0 \qquad -\infty < x < \infty \qquad (3)$$

$$u \to 0 \qquad 0 < y < p/2 \qquad x \to \infty \qquad (4)$$

$$u = \exp(-x) \qquad y = p/2 \qquad 0 < x < b \qquad (5)$$

$$\partial u/\partial y = 0 \qquad y = p/2 \qquad b < x < \infty \qquad (6)$$

where b is $Bp/2L$ and B is the axial length of the heating section. The conditions that typify model (i) are:

$$u \to 0 \qquad 0 < y < p/2 \qquad x \to -\infty \qquad (7)$$

$$\partial u/\partial y = 0 \qquad y = p/2 \qquad -\infty < x < 0. \qquad (8)$$

For model (ii) condition (7) together with the following holds

$$u = 0 \qquad y = p/2 \qquad -\infty < x < 0 \qquad (9)$$

For the more simplified model (iii) only the following condition is prescribed

$$u = 0 \qquad 0 < y < p/2 \qquad x = 0. \qquad (10)$$

Note that for all three models the boundary conditions are mixed. The analyses will be constructed by assuming the flux, $\partial u/\partial y$, on $y = p/2$ $0 < x < b$ or $-\infty < x < b$ is a known function $f(x)$. Fourier Integral type of solutions for u are then obtained in terms of f. Finally by imposing the condition on u along $y = p/2$, $0 < x < b$ or $y = p/2$ $-\infty < x < b$ one gets a Fredholm type of integral equation which governs f. There are a number of ways to solve the latter, of which the easiest is to transform the integral equation into a set of algebraic linear equations.

For models (i) and (iii) the solutions are simpler when the flux is prescribed along the heating surface. In such cases the following conditions hold on the heating surface.

$$\partial u/\partial y = \exp(-x) \qquad y = p/2 \qquad 0 < x < b. \quad (5')$$

Thus the flux is prescribed over the entire range $-\infty < x < \infty$ so that the boundary conditions

are no longer of the mixed type. For these two models $f(x)$ in known *a priori* to be equal to $\exp(-x)$.

Model (ii) is solved by defining $f(x)$ for the range $-\infty < x < 0$ and obtaining a Fredholm type of integral equation for it.

SOLUTIONS

If the method of separation of variables is used in the treatments of model (i) and (ii) one finds that the general solution of equation (2) which satisfies condition (3) has the form

$$u = \int_{-\infty}^{\infty} A(\lambda)\cosh\left[\sqrt{(\lambda^2+1)}y\right]\exp(i\lambda x)\,d\lambda. \quad (11)$$

Differentiating with respect to y and substituting $y = p/2$ and equating the derivative to $f(x)$, one finds that $A(\lambda)$ is governed by the following integral equation:

$$f(x) = \int_{-\infty}^{\infty} A(\lambda)\sqrt{(\lambda^2+1)}\sinh\left(\sqrt{(\lambda^2+1)}p/2\right) \times \exp(i\lambda x)\,d\lambda. \quad (12)$$

Then by using the properties of the Fourier Integrals the last relationship is inverted. It is thus found that u is given by

$$u = \int_a^c K(x,y,\xi)f(\xi)\,d\xi \quad (13)$$

where a and c, the upper and lower limits vary from case to case (see Table 1). The Kernel is given by

$$K = \frac{1}{2\pi}\int_{-\infty}^{\infty} \frac{\cosh\left[\sqrt{(\lambda^2+1)}y\right]e^{i\lambda(x-\xi)}}{\sqrt{(\lambda^2+1)}\sinh\left[\sqrt{(\lambda^2+1)}p/2\right]}\,d\lambda \quad (14)$$

and it can be easily calculated because the integrand has simple poles along the imaginary axis in the complex λ plane at

$$\lambda_n = \pm i\sqrt{(1+4n^2\pi^2/p^2)} = \pm i\beta_n \qquad n = 0, 1, 2, \ldots.$$

Therefore, by appending to the integral along the real axis an integral along a very large arch in the upper or the lower half of the λ plane and utilizing the Cauchy Theorem one gets

$$K = \frac{1}{p}\exp(-|x-\xi|) + \frac{2}{p}\sum_{n=1}^{\infty}\frac{\cos(2n\pi y/p)\exp(-|x-\xi|\beta_n)}{(-1)^n\beta_n}. \quad (15)$$

The extension of this solution to model (iii) is immediate. In view of condition (10) the expression for u is written as follows

$$u = \int_0^{\infty} B(\lambda)\cosh\left[\sqrt{(\lambda^2+1)}y\right]\sin(\lambda x)\,d\lambda. \quad (11')$$

Using the properties of the Fourier Sine transform one finds that in this case too the form (13) holds. However for model (iii) K is given by

$$K = \frac{1}{p}[\exp(-|x-\xi|) - \exp(-|x+\xi|)] + \frac{2}{p}\sum_{n=1}^{\infty}\frac{\exp(-\beta_n|x-\xi|)-\exp(-\beta_n|x+\xi|)}{(-1)^n\beta_n} \times \cos\left(\frac{2n\pi y}{p}\right) \quad (16)$$

Equations (13), (15) and (16) represent the solution for u which satisfy the governing equation, the conditions prescribed at $y = 0$, $x \to +\infty$, $x \to -\infty$ and along $b < x < \infty$, $y = p/2$. From the remaining conditions f is obtained. If the conditions are not mixed f is given explicitly. When the conditions are mixed $f(x)$ is governed by

$$u(x,p/2) = \int_a^c f(\xi)K(x,p/2,\xi)\,d\xi \quad (17)$$

where this equation holds over the entire range $-\infty < x < b$ or part thereof. The solution of equation (17) is discussed in the Appendix. All these cases are summarized below.

Note that in the cases when f is given explicitly, ϕ can be obtained by straightforward integration. Thus for model (i) with prescribed constant flux ϕ is given by:

Model	Quantity prescribed on heating surface	Kernel	f is given by
(i)	temperature	(15)	f is obtained from equation (17) with $a = 0 \quad c = b \quad u(x,p/2) = \exp(-x) \quad 0 < x < b$
	flux	(15)	$a = 0 \quad c = b \quad f(x) = \exp(-x) \quad 0 < x < b$
(ii)	temperature	(15)	f is obtained from equation (17) with $a = -\infty \quad c = b \quad u(x,p/2) = \exp(-x) \quad 0 < x < b$; $= 0 \quad -\infty < x < 0$
	flux	(15)	for sub-range $0 < x < b \quad f = \exp(-x)$; for sub-range $-\infty < x < 0$ f is obtained from equation (17) with $a = -\infty \quad c = 0 \quad u(x,p/2) = 0 \quad -\infty < x < 0$
(iii)	temperature	(16)	f is obtained from equation (17) with $a = 0 \quad c = b \quad u(x,p/2) = \exp(-x) \quad 0 < x < b$
	flux	(16)	$a = 0 \quad c = b \quad f = \exp(-x) \quad 0 < x < b$

$$\phi = \frac{2}{p}\left\{\frac{1}{2}x + 1 - e^{-2(b-x)} + \sum_{n=1}^{\infty} \frac{\cos(2n\pi y/p)}{(-1)^n \beta_n}\left[\frac{1 - e^{-x(\beta_n - 1)}}{\beta_n - 1} + \frac{1 - e^{-(b-x)(\beta_n+1)}}{\beta_n + 1}\right]\right\} \quad (18)$$

whereas for model (iii) we obtain

$$\phi = \frac{2}{p}\left\{\frac{1}{2}x - e^{-2(b-x)} + e^{-2b} + \sum_{n=1}^{\infty} \frac{\cos(2n\pi y/p)}{(-1)^n \beta_n}\left[\frac{1 - e^{-x(\beta_n - 1)}}{\beta_n - 1} + \frac{1 - e^{-(b-x)(\beta_n+1)}}{\beta_n + 1} - \frac{e^{-x(\beta_n-1)} - e^{-b(\beta_n+1)-x(\beta_n-1)}}{\beta_n + 1}\right]\right\} \quad (19)$$

Equations (18) and (19) are valid in the range $0 \leqslant x \leqslant b$. If desired, similar expressions can be obtained easily for the range $-\infty$ to 0 and b to ∞.

RESULTS AND DISCUSSION

In the definition of the local Nusselt number use is made of the mean dimensionless temperature which is given by

$$\bar{\phi} = \frac{2}{p}\int_0^{p/2} \phi(x,y)\,dy. \quad (20)$$

Evidently the behavior of this quantity is worth noting. Compact expressions for $\bar{\phi}$ are obtained by going through rather straightforward integration using equations (13), (15) and (16).

$$\bar{\phi} = \frac{1}{p}e^{x}\int_a^b f(\xi)e^{-|x-\xi|}\,d\xi \quad a = 0 \text{ for model (i) and } -\infty \text{ for (ii)} \quad (21)$$

$$\bar{\phi} = \frac{1}{p}e^{x}\int_0^b f(\xi)[e^{-|x-\xi|} - e^{-|x+\xi|}]\,d\xi \quad \text{for model (iii).}$$

Surprisingly both expressions are independent of x for $x > b$ and while this must be so when axial conduction is neglected this result is not that obvious in the case under discussion. Indeed if heat is transferred only by convection $\rho UC_p\bar{\phi}$ is proportional to Q, the total x directed heat transferred along the duct. Since the duct leading out of the heating section is insulated that quantity must be independent of x. However when axial conduction is effective the total x directed heat flux is given by the following relationship

$$Q \propto \rho UC_p \int_0^{p/2} \left(2\phi - \frac{\partial\phi}{\partial x}\right) dy. \tag{23}$$

Thus constancy of Q does not imply constancy of $\bar{\phi}$ unless the total x-directed diffusion vanishes. Evidently this is what happens. This means that conduction near the walls and at the core are in opposite directions and in complete balance.

The local Nusselt number is defined by the following relationship

$$Nu \equiv \frac{L(\partial T/\partial y)_w}{T_w - \bar{T}} = \frac{(p/2)(\partial\phi/\partial y)_w}{\phi_w - \bar{\phi}} \tag{24}$$

where the subscript w implies that the quantity is evaluated at the heating surface. Thus, when the temperature and flux are prescribed ϕ_w and $(\partial\phi/\partial y)_w$, respectively, are equal to unity. In Figs. 2–7, Nu is plotted as a function of the axial distance. In these, the Péclét number p and the dimensionless length b/p^2 serve as parameters. Thus these figures contain a sizeable amount of information about the influence of the axial diffusion.

It is useful to compare the results obtained here with the available ones for very large Péclét number. Under such circumstances the

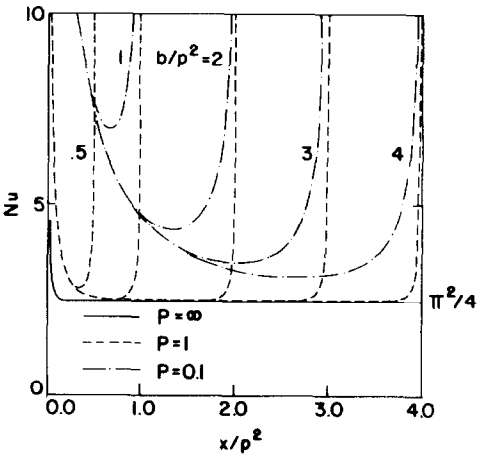

FIG. 3. Local Nusselt number for model (ii), T_w = const.

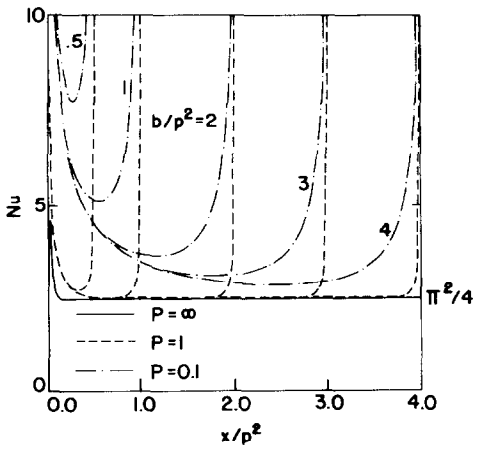

FIG. 2. Local Nusselt number for model (i), T_w = const.

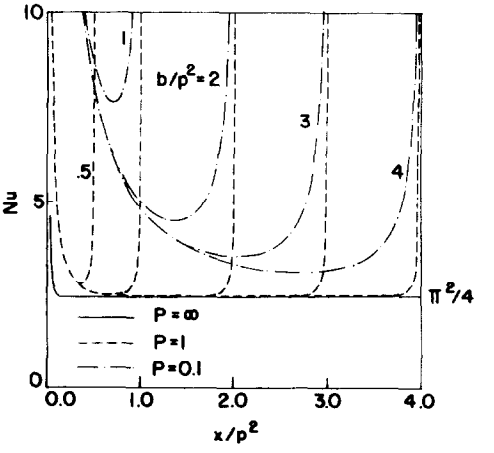

FIG. 4. Local Nusselt number for model (iii), T_w = const.

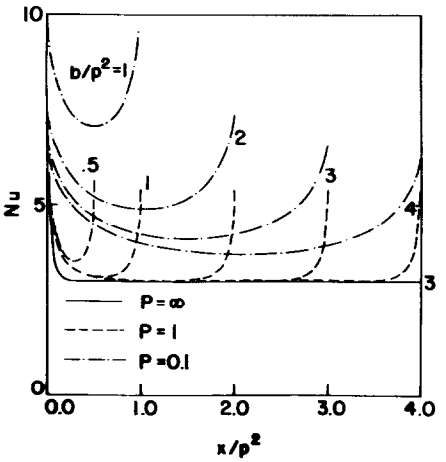

FIG. 5. Local Nusselt number for model (i), q_w = const.

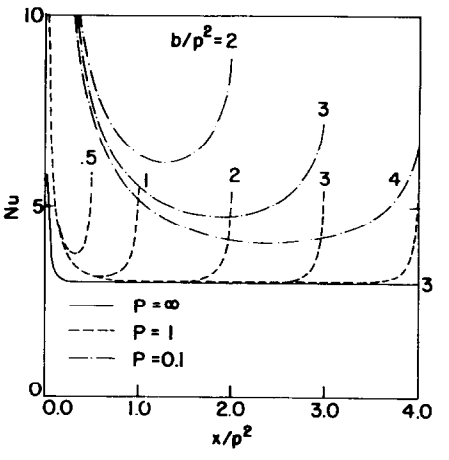

FIG. 7. Local Nusselt number for model (iii), q_w = const.

effect of axial conduction is negligible and the solution for prescribed flux and prescribed temperature are given, respectively, by

$$\phi = 1 - \frac{4}{\pi}\sum_{m=0}^{\infty}\frac{(-1)^m}{2m+1}\cos\left(\frac{(2m+1)\pi y}{p}\right) \times \exp\left(-\frac{(2m+1)^2\pi^2 x}{2p^2}\right) \qquad (25)$$

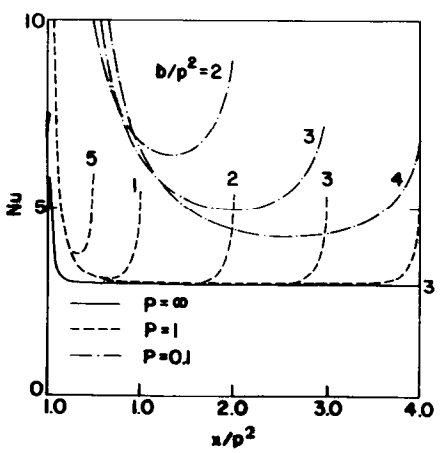

FIG. 6. Local Nusselt number for model (ii), q_w = const.

and

$$\phi = \frac{x}{p} + \frac{y^2}{p} - \frac{p}{12} - \frac{p}{\pi^2}\sum_{n=1}^{\infty}\frac{(-1)^n}{n^2} \times \cos\left(\frac{2n\pi y}{p}\right)\exp\left(-\frac{2n^2\pi^2 x}{p^2}\right) \qquad (26)$$

for the range $0 < x < b$. Evidently the expressions for the local Nusselt numbers formed using these solutions are functions of x/p^2 for any p. In other words, when plotted as functions of x/p^2, the group of curves for all Nusselt numbers collapse onto one provided p is sufficiently high and axial conduction is neglected. They are symbolically designated by $p = \infty$. This is so both in the case of prescribed flux and in the case of prescribed temperature. Therefore the effect of axial diffusion can be conveniently studied if the variable x/p^2 is adopted as the abcissa for all curves.

The curves representing the local Nusselt number for $p = \infty$ asymptote $\pi^2/4$ and 3 for the cases of prescribed temperature and prescribed flux, respectively. The local Nusselt number is higher if axial conduction is taken into account, and substantially so, if the Péclét number is less than unity or when the duct is short.

While the curves representing Nu vs. x/p^2 for $p = \infty$ decrease monotonically the curves for the cases in which axial conduction is accounted for are U shaped. For the case of the prescribed constant wall temperature the Nu approaches infinity at $x = 0$ and $x = b$. Thus Nu is unbounded not only where there is a step change in the prescribed temperature but also where the heating section is connected to the insulated section. When constant flux is prescribed Nu is finite at $x = b$. At $x = 0$ Nu is finite for model (i), infinite for model (iii) and for model (ii) it approaches infinity at some point $x_0 > 0$ and is negative in the narrow region $0 < x < x_0$ (not seen in Fig. 6). The reason for this is because the wall temperature approaches zero for $x \to 0$ and $\bar{\phi}$ is higher than ϕ_w in this region. Comparison between the results for the various models indicates that the local Nusselt number is lowest for model (i). The values of Nu for models (ii) and (iii) are close, but that of model (iii) are generally slightly higher. Both these results as well as those discussed below become understandable if one treats the surfaces or regions where T is equal to T_0 as a heat sinks. That sink is way out at $x = -\infty$ in case (i), it reaches quite close to the heating section yet extends to $x = -\infty$ in model (ii) and it is downright at the inlet in model (iii). The case of model (ii) with constant heat flux is, however, somewhat exceptional. Close to the origin Nu is negative for model (ii), i.e. less than for model (iii). On the other hand for large x (as seen in Figs. 6 and 7) Nu for model (ii) is slightly higher.

For negligible axial diffusion the local Nusselt number provides a measure of the heat transfer efficiency from the heating surface into the fluid. It could be integrated to yield an average heat transfer coefficient for the calculation of the heat absorbed by the fluid. However, when axial diffusion is present this is not necessarily true. For a given heating surface we will usually be interested in its capability to increase the fluid temperature (or concentration) at the outlet. This is best represented for the case of constant wall temperature by the average heat transfer coefficient in the commonly used equation

$$Q = \bar{h}S\frac{(T_w - T_0) - (T_w - \overline{T(\infty, y)})}{\ln (T_w - T_0)/[T_w - \overline{T(\infty, y)}]}. \quad (27)$$

In this equation Q is the total heat absorbed by the fluid and not necessarily the heat transferred from the heating surface.

The heat provided by the heating section may be substantially larger due to "loss" to the heat sinks. Note also that the use of equation (27) is somewhat modified as compared to its use when axial diffusion is absent. At the inlet the temperature difference $(T_w - T_0)$ is used instead of the conventional $(T_w - \overline{T(0, y)})$. Likewise at the outlet we use $(T_w - \overline{T(\infty, y)})$ instead of $(T_w - \overline{T(b, y)})$. (Incidently it was shown that $\overline{T(\infty, y)}$ and $\overline{T(b, y)}$ are equal.) This definition seems to be a natural generalization of the case where axial diffusion is ignored. $\overline{Nu}$, the average Nusselt number based on $\bar{h}$, is given by

$$\overline{Nu} \equiv \frac{\bar{h}L}{k} = -\frac{p^2}{2b}\ln (1 - \overline{\phi(\infty, y)}). \quad (28)$$

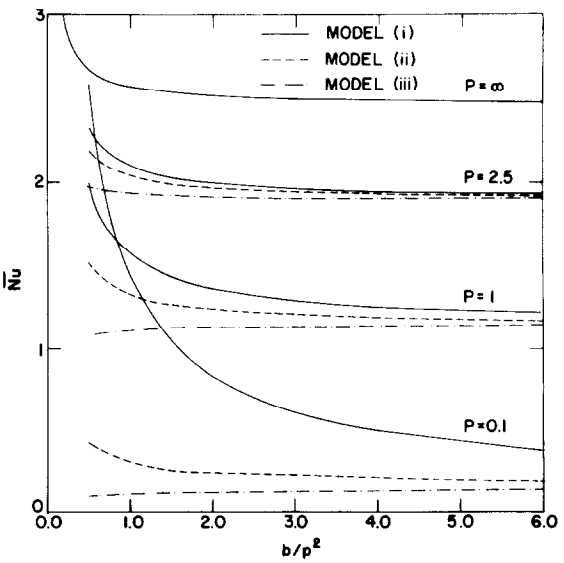

FIG. 8. Average Nusselt number as a function of the heating region length and the Péclét number.

The values of $\overline{Nu}$ for various Péclét numbers and heating lengths is plotted in Fig. 8. Note that provided the duct is sufficiently long $\overline{Nu}$ increases with p and reaches its highest value for the case of negligible streamwise diffusion. The decrease of $\overline{Nu}$ with decreasing p represents the effect of heat "lost" by conduction to the upstream sinks if they are finite distance away. Also whether the sinks are close or far upstream they tend to keep the heat in the heating section rather than have it washed away. Thus the temperature difference in the heating section is small and the heating becomes less efficient. As expected for given p and b, $\overline{Nu}$, is highest for model (i) and lowest for (iii). For long heating sections the average Nusselt number approaches a constant which is equal for all three models.

For the case of prescribed constant heat flux $\overline{\phi(\infty, y)}/p$ is plotted as a function of the heating length (see Fig. 9). For negligible axial conduction, $p = \infty$, the curve is a straight line. This expresses the fact that all the heat supplied to the system is absorbed by the fluid. One gets an identical curve for model (i) because in this case there is no loss to the surroundings. For models (ii) and particularly (iii) appreciable amount of heat is lost resulting in a substantial decrease in ϕ.

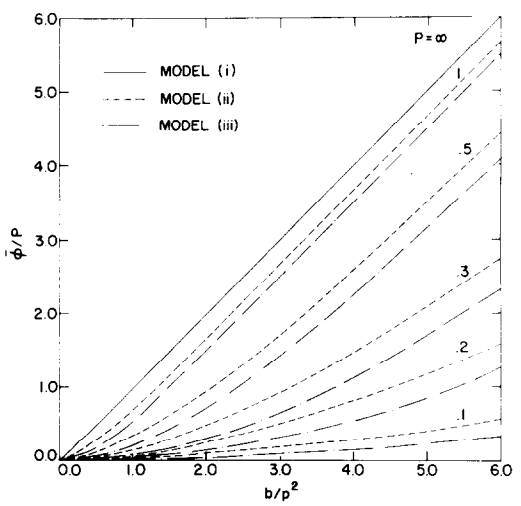

FIG. 9. Mean temperature as a function of the heating region length and the Péclét number, q_w = const.

ACKNOWLEDGEMENT

The computations connected with this paper were performed at the computation center of the Tel-Aviv university. The writers thanks Mrs. D. Neulander for her assistance in obtaining the numerical results presented in this paper.

REFERENCES

1. Z. ROTEM and J. E. NEILSON, Exact solution for diffusion to flow down an incline, *Can. J. Chem. Engng* **47**, 341–346 (1969).
2. S. N. SINGH, Heat transfer by laminar flow in a cylindrical tube, *Appl. Sci. Res.* **A7**, 325–340 (1958).
3. KH. BOYADZHIEV, V. LEVITCH and V. KRYLOV, Improving the theory of convection diffusion, *Int. Chem. Engng* **8**, 341–346 (1969).
4. C. HSU, An exact mathematical solution for entrance-region laminar heat transfer with axial conduction, *Appl. Sci. Res.* **A17**, 359–376 (1967).
5. P. J. SCHNEIDER, Effect of axial fluid conduction on heat transfer in the entrance regions of parallel plates and tubes, *Trans. Am. Soc. Mech. Engrs* **79**, 765–773 (1957).
6. C. HSU, An exact analysis of low Péclét number thermal entry region heat transfer in transversely nonuniform velocity field, *A.I.Ch.E. Jl* **17**, 732–740 (1971).
7. C. HSU, Theoretical solution for low-Péclét-number, thermal-entry-region heat transfer in laminar flow through concentric annuli, *Int. J. Heat Mass Transfer* **13**, 1907–1924 (1970).
8. A. S. JONES, Extensions to the solution of the Graetz Problem, *Int. J. Heat Mass Transfer* **14**, 619–623 (1971).

APPENDIX

Numerical Solution of the Integral Equations

In splitting the range $a < x < c$ to finite intervals and converting the Fredholm integral equation (17) to a set of equations and unknowns care must be exercised. Note that both K and the solution f contain singular points. Indeed by setting $y = p/2$ in equations (15) and (16) and approximating β_n by $n\pi$, one finds that the summation in the expressions for K diverge for $\xi = x$. Also the singularity of f at $x = 0$ and $x = b$ has been discussed. However both singularities have limited influence on the finite difference scheme if the integral equation (17), considering model (iii) as an example, is converted to

$$\sum_{j=1}^{n} H_{ij} f_j = u_i \qquad \text{(A.1)}$$

where

$$f_j = f[(j - \tfrac{1}{2})\Delta x] \qquad i = 1, 2, \ldots n \qquad \text{(A.2)}$$

$$u_i = u[(i - \tfrac{1}{2})\Delta x, p/2] \quad \text{(A.3)}$$

$$H_{ij} = \int_{(j-1)\Delta x}^{j\Delta x} K[(i - \tfrac{1}{2})\Delta x, p/2, \eta]\, d\eta \quad j = 1, 2, \ldots n. \quad \text{(A.4)}$$

These relationships imply that the range $0 < x < b$ is split into n intervals and the sets of equations (A.1) produce solutions for the value of f at the mid points of these intervals. Thus $f(0)$ and $f(b)$, which may be singular, do not constitute the unknowns of the algebraic problem defined by the last four equations. Also although K is unbounded for $\xi = x$, H_{ij} is bounded for $i = j$.

The calculations of the elements in the matrices H_{ij} is fairly straightforward. However it is well worth recording a development which allows for a considerable saving of computer time. Let K^- be given by

$$K^- = \frac{1}{p} e^{-r} + \frac{2}{p} \sum_{n=1}^{\infty} \frac{e^{-r\beta_n}}{\beta_n} \quad \text{(A.5)}$$

where r is $|x - \xi|$. Also let K^+ be given by the same expression except that r is $|x + \xi|$. A vector H_i is constructed. Its components are the areas under the curve $K^-(r)$ shown in Fig. A.1. One can show that these components are given by

$$H_1 = \frac{2}{p}\left[1 - e^{-\Delta x/2} + 2 \sum_{n=1}^{\infty} \frac{1 - e^{-\beta_n \Delta x/2}}{\beta_n^2}\right] \quad \text{(A.6)}$$

$$H_i = \frac{2}{p}\left[e^{-r_i} \sinh\left(\frac{\Delta x}{2}\right) + 2 \sum_{n=1}^{\infty} \frac{e^{-r_i \beta_n} \sinh(\beta_n \Delta x/2)}{\beta_n^2}\right] \quad i > 1 \quad \text{(A.7)}$$

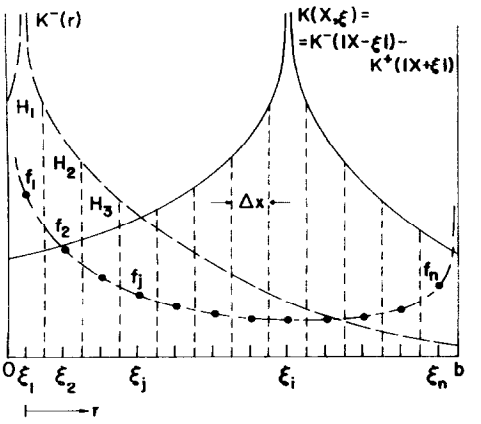

FIG. A1. Scheme of the numerical discretization.

where $r_i = (i - 1)\Delta x$ $i = 1, \ldots n$. In view of the symmetry of K^+ and K^- the elements in the matrix H_{ij} is

$$H_{ij} = H_{|i-j|+1} + H_{i+j}.$$

Note that the vector H_i contain n terms while the matrix H_{ij} contains n^2 terms. Hence, a considerable saving in the number of operations is achieved.

EFFET DES CONDITIONS AUX LIMITES EN AMONT ET EN AVAL SUR LE TRANSFERT THERMIQUE (OU MASSIQUE) AVEC DIFFUSION AXIALE

Résumé—Les auteurs étudient systématiquement le rôle des conditions aux limites en amont et en aval sur le transfert thermique (ou massique) quand la diffusion axiale est effective. On a considéré trois cas similaires d'écoulements établis en conduite. Dans tous les cas, il existe une section centrale chauffante et les fluides s'écoulent depuis celle-ci à l'intérieur d'une conduite isolée semi-infinie. Les configurations réalisées en amont de cette section varient.

Comme attendu on trouve que ces configurations ont une forte influence quand le nombre de Péclet est faible et la section chauffante courte.

L'analyse menée en admettant un profil d'écoulement uniforme n'est néanmoins pas passée car, dans les trois cas, les conditions aux limites sont mixtes. Des solutions sont obtenues sous la forme d'intégrales de Fourier dont l'inversion est faite numériquement.

AUSWIRKUNGEN VON STROMAUFWÄRTS UND STROMABWÄRTS VORLIEGENDEN RANDBEDINGUNGEN AUF DEN WÄRME- (STOFF-) TRANSPORT MIT AXIALER LEITUNG (BZW. DIFFUSION)

Zusammenfassung—Die Autoren untersuchen systematisch die Rolle von stromaufwärts und stromabwärts vorliegenden Randbedingungen auf den Wärme- (oder Stoff-) Transport, wenn in Achsrichtung Leitung bzw. Diffusion wirkt. Als Beispiel werden drei ähnliche Fälle der Pfropfenströmung in Kanälen behandelt. Bei all diesen Fällen wird ein mittlerer Kanalabschnitt beheizt und das Fluid strömt danach in einen halbunendlichen adiabaten Kanal. Die Bedingungen stromaufwärts vor dem Heizabschnitt sind

Wie erwartet, ergibt sich, dass diese Bedingungen einen wesentlichen Einfluss haben, wenn die Péclet-Zahl klein und der beheizte Kanalabschnitt kurz ist.

Die Untersuchung wurde unter Annahme eines gleichförmigen Geschwindigkeitsprofils durchgeführt. Dies ist dennoch ziemlich kompliziert, weil in allen drei Fällen die Randbedingungen gemischt sind. Die Lösungen liegen in Form von Fourier-Integralen vor, deren Auswertung numerisch durchgeführt wurde.

ВЛИЯНИЕ ГРАНИЧНЫХ УСЛОВИЙ ВВЕРХ И ВНИЗ ПО ТЕЧЕНИЮ НА ТЕПЛО- И МАССОПЕРЕНОС ПРИ НАЛИЧИИ ДИФФУЗИИ ВДОЛЬ ОСИ

Аннотация—Исследуется влияние граничных условий вверх и вниз по течению на теплоперенос (или массоперенос) при наличии существенной диффузии вдоль оси. В качестве примеров изучаются три подобных типа стержневого течения в каналах. Во всех этих случаях имеется центральный участок нагрева, откуда жидкость течет в изолированный полуограниченный трубопровод. Определяющие условия в верхней части этого участка изменяются.

Как и предполагалось, эти условия оказывают существенное влияние на теплоперенос при малых числах Пекле и малой длине участка нагрева.

Анализ проводился в предположении, что профиль течения равномерный, но отличный от прямого, так как во всех трех случаях граничные условия являются смешанными. Решения получены в виде интегралов Фурье, обращение которых проводится численным путем.